

Hydrogenation-Induced Insulating State in the Intermetallic Compound LaMg_2Ni

K. Yvon,¹ G. Renaudin,¹ C. M. Wei,² and M. Y. Chou³

¹Laboratory of Crystallography, University of Geneva, 1211 Geneva 4, Switzerland

²Institute of Physics, Academia Sinica, Nankang, Taipei, Taiwan 11529, Republic of China

³School of Physics, Georgia Institute of Technology, Atlanta, Georgia 30332-0430, USA

(Received 12 August 2004; published 18 February 2005)

Hydrogenation-induced metal-semiconductor transitions usually occur in simple systems based on rare earths and/or magnesium, accompanied by major reconstructions of the metal host (atom shifts $>2 \text{ \AA}$). We report on the first such transition in a quaternary system based on a transition element. Metallic LaMg_2Ni absorbs hydrogen near ambient conditions, forming the nonmetallic hydride $\text{LaMg}_2\text{NiH}_7$ which has a nearly unchanged metal host structure (atom shifts $<0.7 \text{ \AA}$). The transition is induced by a charge transfer of conduction electrons into tetrahedral $[\text{NiH}_4]^{4-}$ complexes having closed-shell electron configurations.

DOI: 10.1103/PhysRevLett.94.066403

PACS numbers: 71.30.+h, 61.66.Fn, 71.15.Mb, 72.80.Ga

Hydrogenation-induced metal-nonmetal transitions occur in relatively simple systems based on nontransition elements such as yttrium (Y-YH_{3-x}) and analogues, or main-group elements such as magnesium (Mg-MgH_2) [1,2]. For transition (T) elements the only well documented example is the nickel based ternary system $\text{Mg}_2\text{Ni-H}$. Upon hydrogenation the metallic compound Mg_2Ni transforms into a nonmetallic hydride of stoichiometric composition Mg_2NiH_4 that shows optical mirror properties [3] and provides a safe way of storing hydrogen [4]. The nature of the electron correlations leading to these transitions is of fundamental interest and subject of current research (see, e.g., [5]). One reason why these correlations are still poorly understood is the fact that they are accompanied by major reconstructions of the metal atom arrangements. In the Mg-H system, for example, the Mg atom arrangement changes from hexagonal close packed in metallic Mg to tetragonal in nonmetallic MgH_2 . In the La-H and Y-H systems the hydrogenation-induced changes in the close-packed metal substructures are somewhat smaller, but on a local level, in particular, around hydrogen defects, they are substantial [6]. Finally, in the $\text{Mg}_2\text{Ni-H}$ system the metal-nonmetal transition leads to atomic shifts of up to 2 \AA and a breaking of metal-metal bonds.

Metal-nonmetal transitions in T-metal-hydrogen systems without reconstruction of the metal substructure have not yet been reported. Here we report on the first such transition in the nickel based system $\text{LaMg}_2\text{Ni-H}$. Intermetallic LaMg_2Ni absorbs reversibly hydrogen near ambient conditions hereby forming an ordered stoichiometric hydride of composition $\text{LaMg}_2\text{NiH}_7$ [7]. Hydrogen enters various types of interstices in, but does not lead to a reconstruction of, the metal substructure. In this combined experimental and theoretical work we show that the hydride is nonmetallic and that the electron correlations responsible for the metal-nonmetal transition are presumably identical to those leading to the formation of T-metal-

hydrogen “complexes” having closed-shell electron configurations.

Hydrogen-free LaMg_2Ni crystallizes with orthorhombic symmetry [8]. Its structure contains a distorted hexagonal honeycomb network of short metal-metal bonds ($\text{La-Ni} = 2.95$ and 3.05 \AA , parallel to the a - b plane) in which Mg atoms are inserted (Fig. 1). The hydride $\text{LaMg}_2\text{NiH}_7$ forms readily below $200 \text{ }^\circ\text{C}$ and 8 bar hydrogen pressure and crystallizes with monoclinic symmetry [8]. It is stoichiometric and shows no homogeneity range. Similar to “interstitial” hydrides its metal atom arrangement does not much differ from that of the alloy. It expands in the a - b plane, contracts slightly along c , and undergoes a small monoclinic lattice distortion (deviation from orthogonality

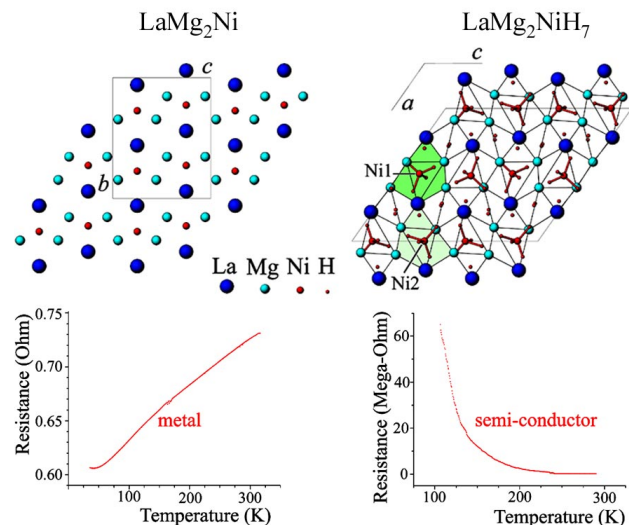


FIG. 1 (color online). Structure and resistance of orthorhombic LaMg_2Ni (a) and monoclinic $\text{LaMg}_2\text{NiH}_7$ (b) as measured on compacted polycrystalline samples. Tetrahedral $[\text{NiH}_4]^{4-}$ complexes and H^- anions are shown; short La-Ni bonds in alloy \parallel a - b plane.

$<0.3^\circ$). While the expansion ($\Delta V/V \sim 19\%$) leads to a general increase in metal-metal bond lengths (La-Ni = 3.17–3.62 Å) all atom shifts remain below 0.7 Å [8]. Hydrogen is located on 14 different fully occupied interstitial sites of which six are coordinated by lanthanum and magnesium atoms only. Of particular interest for the electronic structure are the hydrogen configurations around the transition element. In fact, both nickel atoms are surrounded by four hydrogen atoms in ordered tetrahedral configurations (Fig. 1). Thus, from a bonding point of view the structure can be rationalized in terms of two nickel centered tetrahedral metal-hydrogen complexes of limiting ionic formula $[\text{NiH}_4]^{4-}$, and of six hydrogen anions H^- surrounded by Mg^{2+} and La^{3+} cations only. While hydrogen in the complexes (called “complex” hydrogen from here on) interacts strongly with nickel (D-Ni = 1.49–1.64 Å), hydrogen outside the complexes (called interstitial hydrogen from here on) interacts with magnesium (Mg-D = 1.82–2.65 Å) and lanthanum (La-D = 2.33–2.59 Å) only. The bond distances with nickel correspond to the sum of covalent radii ($0.38 + 1.1 = 1.48$ Å) while those with lanthanum and magnesium are consistent with, but occasionally shorter than, those in the corresponding saline binary hydrides (MgD_2 : 1.95 Å, LaD_3 : 2.43 Å). Thus the metal-hydrogen bonds are expected to have more covalent (i.e., directional) character for nickel (presumably of sp^3 type) and more ionic character for lanthanum and magnesium. This bonding description implies a charge transfer from La and Mg to both complex and interstitial hydrogen such that the Ni d bands are nearly filled and all valence electrons are localized around hydrogen. In other words, the hydride should be nonmetallic. In order to give support for this model, resistance measurements and first-principles calculations were performed.

The resistance measurements were done by the four-contact technique on pressed powders of both intermetallic LaMg_2Ni and its hydride $\text{LaMg}_2\text{NiH}_7$. Parallelepipeds of $10 \times 3 \times 1$ mm³ size were prepared under argon atmosphere in a glove box, and voltage and current leads were attached by using silver paint. The samples were mounted on an electrically insulating support, and then attached to the cold finger of a cryocooler. The temperature was measured using a Cernox thermometer. The range of dc currents was 1×10^{-4} – 1×10^{-8} A; the current was first applied in one direction and was then reversed, in order to eliminate thermal emf effects. Data were recorded from room temperature to 10 K in steps of 5 K. As can be seen in the lower part of Fig. 1 they show the expected metallic behavior for the intermetallic compound and the expected semiconducting behavior for the hydride. It is difficult to extract the exact bulk resistivity from electrical measurements on compressed powder samples, since a contribution from oxides between the grains cannot be avoided.

Theoretical calculations were carried out using the Vienna *ab initio* simulation package (VASP) based on

density functional theory and the projector augmented wave method (PAW) with plane waves [9]. The generalized gradient approximation (GGA) was used. The energy cut-off is 269.6 eV and the k -point set used was $8 \times 4 \times 4$ for LaMg_2Ni and $4 \times 8 \times 4$ for $\text{LaMg}_2\text{NiH}_7$, respectively. The outer core shells (5s and 5p) of La were included as valence states. All calculated lattice constants were within 1–2% of the experimental values.

The projected density of states (PDOS) plot of metallic LaMg_2Ni is shown in Fig. 2(a). The peak around 1–2 eV below the Fermi level, E_F , is associated with the Ni d band, while the peak around 2 eV above E_F is associated with the (unoccupied) La f bands. The plot shows a normal metal, although the Ni d bands are much narrower than those in the Ni metal. In comparison, the plot for the hydride $\text{LaMg}_2\text{NiH}_7$ is shown in Figs. 2(b) and 2(c) [10]. A gap appears upon hydrogenation. These plots represent averages over the various atoms sites. The peaks in the range from 0 to –2.0 eV are associated with Ni d states, while those around +2.0 eV are associated with La f states. The

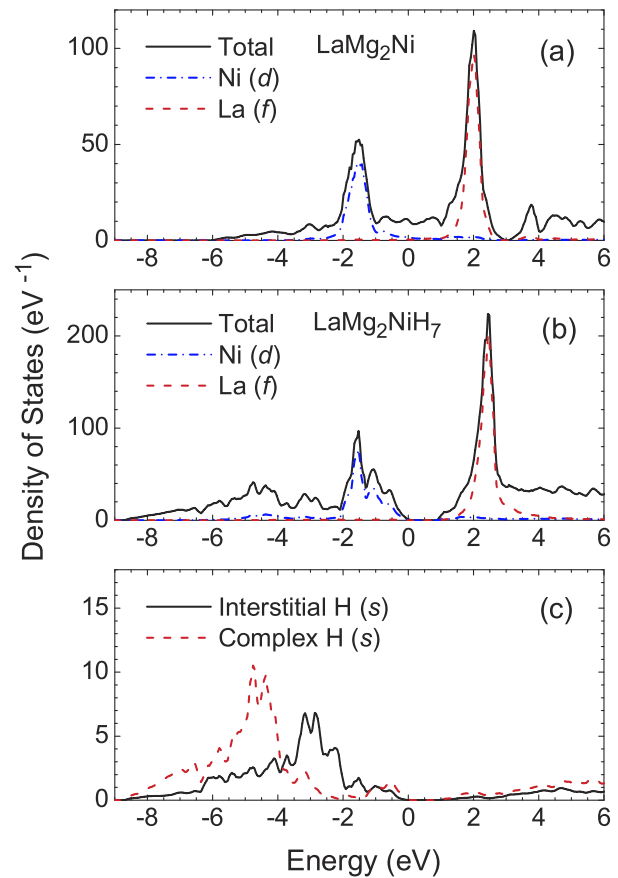


FIG. 2 (color online). (a) Density of states for LaMg_2Ni . The projected density of states for Ni d and La f is also shown, with projection radii of 1.8 Å for La, and 1.2 Å for Ni, respectively. (b) Total density of states and projected density of states of $\text{LaMg}_2\text{NiH}_7$ for Ni d and La f . (c) Projected density of states for interstitial and complex hydrogen with a projection radius of 0.7 Å.

fundamental gap (indirect, Γ to A or Γ to Y) is about 0.9 eV. This is the GGA value, which is expected to be smaller than the quasiparticle gap. A correction of the order of +0.5 to +1.0 eV is expected. One can identify three broad peaks for the occupied states. They can be associated with states (in the order of rising energy) from H- s in the complex, H- s interstitial, and Ni- d , respectively. Almost all the Ni- d states are below the gap, indicating an approximately closed d shell. An examination of the charge density (not shown) concludes that magnesium behaves like an electron donor with very little valence charge in its vicinity, while both types of hydrogen attracts charge as expected from its relatively large electronegativity.

In order to understand the bonding within the tetrahedral $[\text{NiH}_4]^{4-}$ complex, in Fig. 3 we plot the difference between the charge density in the crystal and the superposition of the atomic charge density in a plane containing Ni and two H. This contour plot indicates the charge transfer that takes place when the complex is formed from atoms. The contour interval is $0.05 e/\text{\AA}^3$, with solid (dashed) lines representing positive (negative) changes. The contours show a charge redistribution of the Ni d shell compared to the atom, and, most significantly, an increase of charge density near the H sites. It is interesting to note that the maximum of this increase is not exactly located at the H site. Instead, it is shifted along the H-Ni direction, thus confirming the directional character of the Ni-H interactions.

Summarizing, our theoretical calculations and experimental results on the $\text{LaMg}_2\text{Ni-H}$ system confirm the

occurrence of a hydrogenation-induced charge transfer and the opening of a band gap. The results suggest a filled d band situation and two sorts of metal-hydrogen interactions, a more covalent one involving sp^3 bonded $[\text{NiH}_4]^{4-}$ complexes having closed 18-electron shells (ten Ni $3d$ and four H s , plus four valence electrons formally transferred from Mg to the complex) forming four directional 2-center 2-electron ($2c-2e$) bonds, and a more ionic one involving H^- anions and Mg^{2+} and La^{3+} cations only, as shown by the limiting ionic formula $\text{La}^{3+}2\text{Mg}^{2+}[\text{NiH}_4]^{4-}3\text{H}^-$. This demonstrates that hydrogen contents and H atom distributions in certain T-metal-hydrogen systems can be rationalized in terms of simple electron counting (18-electron rule) and $s-p-d$ hybridization schemes (sp^3).

Apart from the present $\text{LaMg}_2\text{Ni-H}$ system only two other T-metal-hydrogen systems show a similar behavior, including hydrogenation-induced metal-semiconductor and metal-hydrogen complex formation (see Table I). The historically first one concerns the nickel based system $\text{Mg}_2\text{Ni-H}$. The hydride Mg_2NiH_4 is nonmetallic, has a calculated band gap of 1.8 eV [11] and derives from metallic Mg_2Ni by a relatively important rearrangement of its hexagonal metal substructure (Ni-Ni bond breaking; atom shift $\sim 2 \text{\AA}$, volume increase $\sim 32\%$). It displays a disordered hydrogen distribution in its cubic high-temperature phase and has been originally classified as an interstitial hydride. It was only after its monoclinic room-temperature structure had been found to contain an ordered array of tetrahedral 18-electron $[\text{NiH}_4]^{4-}$ complexes that it was classified as a so-called complex metal hydride (for a recent review on this class of compounds see [12]).

The Ni-H distances in these complexes (1.54–1.57 \AA) are closely similar to those in the present $\text{LaMg}_2\text{NiH}_7$ and consistent with covalent interactions, but in contrast to the latter, Mg_2NiH_4 contains no anionic hydrogen surrounded by magnesium cations only. The second example is the recently reported iridium based system $\text{Mg}_3\text{Ir-H}$ [13]. The stoichiometric hydride $\text{Mg}_6\text{Ir}_2\text{H}_{11}$ derives from the intermetallic compound Mg_3Ir by a relatively important rearrangement of the metal substructure (atom shifts $\sim 1.9 \text{\AA}$, formation of new metal-metal bonds, volume increase 40%). Hydrogen occupies not less than 26 different interstices, but the structure is better rationalized in terms of four nearly ordered saddlelike $[\text{IrH}_4]^{5-}$ and square-pyramidal $[\text{IrH}_5]^{4-}$ complexes, all formally 18 electrons and displaying directional $2c-2e$ iridium-hydrogen bonds, and five hydride anions H^- surrounded by Mg^{2+} cations only, corresponding to the limiting ionic formula $4\text{Mg}_6\text{Ir}_2\text{H}_{11} = 5\text{MgH}_2 \cdot 19\text{Mg}^{2+} \cdot 2[\text{IrH}_5]^{4-} \cdot 6[\text{IrH}_4]^{5-}$. Although electric properties have not been reported yet the intensely red color of the hydride suggests nonmetallic behavior. As to other nonmetallic metal hydrides showing complex formation such as Mg_2CoH_5 ($[\text{CoH}_5]^{4-}$) and Mg_2FeH_6 ($[\text{FeH}_6]^{4-}$) they do not fall in this class because stable binary compounds “ Mg_2Co ” and “ Mg_2Fe ” do not exist [12].

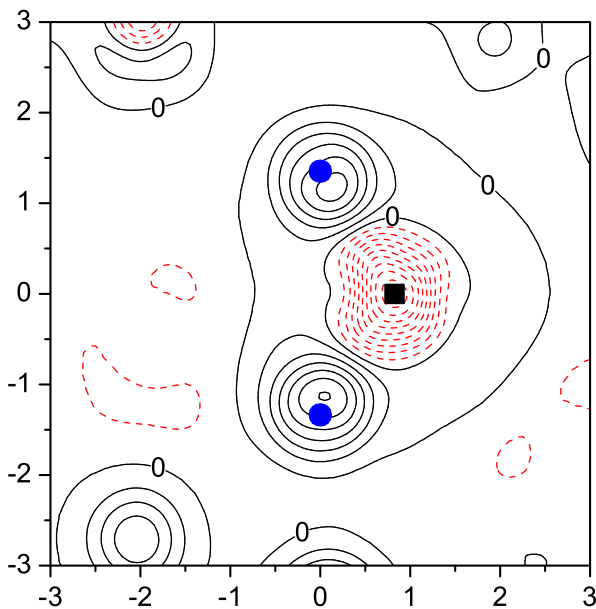


FIG. 3 (color online). Difference charge-density plot of $\text{LaMg}_2\text{NiH}_7$ in the plane containing Ni and 2 H with respect to the superposition of atomic charge densities. Charge deficiency in the plot is represented by dashed lines, while the density increase is plotted by solid lines. The contour increment is $0.05 \text{ electrons}/\text{\AA}^3$. The H positions are indicated by circles, and Ni by a square.

TABLE I. Hydrogenation-induced structural and electronic changes in transition-metal compounds

Compound (symmetry)	Hydride (symmetry)	$\Delta V/V$	Maximum atomic shift	Complexes and H^- anions	Hydride properties
Mg_2Ni (hexagonal)	Mg_2NiH_4 (monoclinic)	32%	$\sim 2.0 \text{ \AA}$	$[NiH_4]^{4-}$	nonmetallic, brownish
Mg_3Ir (hexagonal)	$Mg_6Ir_2H_{11}$ (monoclinic)	40%	$\sim 1.9 \text{ \AA}$	$3[IrH_4]^{5-}$, $[IrH_5]^{4-}$, $5H^-$	nonmetallic, red
$LaMg_2Ni$ (orthorhombic)	$LaMg_2NiH_7$ (monoclinic)	19%	$\sim 0.7 \text{ \AA}$	$[NiH_4]^{4-}$, $3H^-$	nonmetallic, dark gray

Clearly, such simple bonding pictures and electron counting rules cannot be applied to metallic interstitial T-metal hydrides. Given that these usually display wide homogeneity ranges and disordered hydrogen substructures their local hydrogen configurations around the T elements are unknown which precludes their electron requirements from being determined. Nevertheless, for certain systems preferred hydrogen configurations showing directional bonding character do occur, and these can be rationalized in terms of nearly closed-shell electron configurations. Examples are found with $MPdH_{2+x}$ ($M = Ca, Sr, Eu, Yb$) and $MgRhH_{0.94}$. Their CsCl-type metal substructures contain formally 14-electron $[PdH_2]^{2-}$ complexes having linear H-Pd-H bonds, and 48-electron $[Rh_4H_4]^{8-}$ complexes made up by nearly linear Rh-H-Rh bonds in a cyclic squarelike arrangement [12]. The T elements have nearly closed d shells and their H ligands can be rationalized in terms of $2c-2e$ bonds. Even classical hydrogen storage compounds such as $LaNi_5H_7$ show a tendency of forming disordered tetrahedral NiH_4 units whose electron requirements, however, have not yet been estimated. Although none of these systems show hydrogenation-induced metal-nonmetal transitions under the relatively mild pressure-temperature conditions investigated so far, one might speculate that such transitions do occur under more extreme conditions where hydrogenation-induced cell expansion favors electron charge transfer.

In conclusion, our work shows for the first time a hydrogenation-induced metal-nonmetal transition in a quaternary transition-metal-hydrogen system. The transition occurs without major reconstruction of the metal atom network and can be rationalized in terms of a local bonding picture. Insertion of hydrogen leads to a charge transfer of conduction electrons into metal-hydrogen bonds that stabilize T-metal-hydrogen complexes having closed-shell electron configurations. The formation of such complexes, at least on a local level, could be a general phenomenon in metallic interstitial transition-metal hydrides. This could open the door for the discovery of new metal-hydrogen systems showing metal-semiconductor transitions and thus to a better understanding of these transitions.

We thank N. Clayton (Geneva) for help with the resistivity measurements. This work is supported by the Swiss National Science Foundation, the Swiss Federal Office of Energy, the U.S. Department of Energy under Grant No. DE-FG02-97ER45632 (MYC), the U.S. National Science Foundation under Grant Nos. DMR-02-05328

and SBE-01-23532 (MYC), and the National Science Council of Taiwan under Grant No. 92-2112-M001-052 (CMW). The computation used resources of the DOE National Energy Research Scientific Computing Center (NERSC).

- [1] J.N. Huiberts *et al.*, Nature (London) **380**, 231 (1996); R. Griessen, Europhysics News **32**, 41 (2001); K.K. Ng *et al.*, Phys. Rev. Lett. **78**, 1311 (1997).
- [2] For a review on rare-earth hydrides, see P. Vajda, in *Handbook on the Physics and Chemistry of Rare Earths* (Elsevier Science, New York, 1995), Vol. 20, p. 207, and references therein.
- [3] T.J. Richardson *et al.*, Appl. Phys. Lett. **80**, 1349 (2002); J. Isidorsson *et al.*, *ibid.* **80**, 2305 (2002).
- [4] L. Schlapbach and A. Züttel, Nature (London) **414**, 353 (2001); R. C. Bowman Jr. and B. Fultz, MRS Bull. **27**, 688 (2002).
- [5] J.A. Alford *et al.*, Phys. Rev. B **67**, 125110 (2003), and references therein.
- [6] G. Renaudin, K. Yvon, W. Wolf, and P. Herzig (to be published).
- [7] G. Renaudin, L. Guénée, and K. Yvon, J. Alloys Compd. **350**, 145 (2003).
- [8] Crystal data: $LaMg_2Ni$: orthorhombic, space group $Cmcm$, $a = 4.2266(6)$, $b = 10.303(1)$, $c = 8.360(1) \text{ \AA}$, $V = 364.0(1) \text{ \AA}^3$, $Z = 4$, one La, one Mg and one Ni site; $LaMg_2NiH_7$: monoclinic, space group $P2_1/c$, $a = 13.9789(7)$, $b = 4.7026(2)$, $c = 16.0251(8) \text{ \AA}$, $\beta = 125.240(3)^\circ$, $V = 860.39(8) \text{ \AA}^3$, as measured on deuteride; $Z = 8$, two La, four Mg, two Ni and 14 D sites; cell parameter relationship between the alloy (o) and the hydride (m) $\vec{a}_m \cong \vec{b}_o - \vec{c}_o$, $\vec{b}_m \cong -\vec{a}_o$, $\vec{c}_m \cong 2\vec{c}_o$.
- [9] G. Kresse and J. Hafner, Phys. Rev. B **49**, 14251 (1994); G. Kresse and J. Furthmuller, Comput. Mater. Sci. **6**, 15 (1996).
- [10] The projection radii used were 1.8 \AA for La, 1.3 \AA for Mg, 1.2 \AA for Ni, and 0.7 \AA for H. With the small H value, not all the charge was captured, but the energy-distribution trend is visible in these plots.
- [11] E. Orgaz and M. Gupta, Z. Phys. Chem. (Frankfurt/Main) **181**, 1 (1993).
- [12] K. Yvon and G. Renaudin, in "Encyclopedia of Inorganic Chemistry", edited by B. King (John Wiley, New York, to be published); K. Yvon, in "Encyclopedia of Materials: Science and Technology", edited by K.H.J. Buschow (Elsevier Ltd., Oxford, 2004), p. 1.
- [13] R. Cerny, J.M. Joubert, H. Kohlmann, and K. Yvon, J. Alloys Compd. **340**, 180 (2002).